Summary of Investigations into a Laser-Produced Plasma Focused Collisional Radiative Model

N.L. Wong[1], F. O'Reilly[1], E. Sokell[1]

[1] *School of Physics, Science Centre North, UCD, Dublin, Ireland*

The collisional radiative model (CR) presented by Colombant and Tonon [1] is applicable to a variety of plasmas and has often aided more detailed modelling of laser-produced plasmas (LPPs) for source development. Collisional ionization, radiative recombination, and three-body recombination are assumed to be the three dominant processes when the CR model is applied [1]. Eq. (1) shows how the processes can be related at equilibrium to produce a ratio of ion stage populations, and rate coefficients for each process are presented in Eqs. (2–4).

$$\frac{n_{Z+1}}{n_Z} = \frac{S(Z,T_\mathrm{e})}{\alpha_\mathrm{r}(Z+1,T_\mathrm{e}) + n_\mathrm{e}\cdot\alpha_\mathrm{3b}(Z+1,T_\mathrm{e})}, \tag{1}$$

$$S(Z,T_\mathrm{e}) = \frac{9\times10^{-6}\xi_Z(\frac{T_\mathrm{e}}{\chi_Z})^{1/2}}{{\chi_Z}^{3/2}(4.88+\frac{T_\mathrm{e}}{\chi_Z})}\exp(-\frac{\chi_Z}{T_\mathrm{e}}) \quad [\mathrm{cm}^3\cdot\mathrm{s}^{-1}], \tag{2}$$

$$\alpha_\mathrm{r}(Z,T_\mathrm{e}) = 5.2\times10^{-14}(\frac{T_\mathrm{e}}{\chi_Z})^{1/2}Z[0.429+\frac{1}{2}\ln(\frac{\chi_Z}{T_\mathrm{e}})+0.469(\frac{T_\mathrm{e}}{\chi_Z})^{1/2}] \quad [\mathrm{cm}^3\cdot\mathrm{s}^{-1}], \tag{3}$$

$$\alpha_\mathrm{3b}(Z,T_\mathrm{e}) = \frac{2.97\times10^{-27}\xi_Z}{T_\mathrm{e}{\chi_Z}^2(4.88+\frac{T_\mathrm{e}}{\chi_Z})} \quad [\mathrm{s}^{-1}], \tag{4}$$

where n_e is the electron density in cm^{-3}, ξ_Z is the orbital occupancy term equal to the number of electrons in the outermost orbital subshell for an ion of charge Z, χ_Z is the ionization energy for an ion of charge Z in eV, and T_e is the electron temperature in eV. Iteratively solving Eq. (1) for each ion stage at a range of T_es yields curves of relative ion populations in the range of T_es, producing an ion distribution plot. Fig. 1 shows an ion distribution for Xe with two curves labeled as observed ionization bottlenecks (IBs), which are enhanced populations in ion stages predicted to arise at ion stages with full outermost electron orbitals [2].

However, Xe^{5+} and Xe^{7+} correspond to $[Kr]4d^{10}5s^25p^1$, and $[Kr]4d^{10}5s^1$, respectively. Consequently, the observed IBs are contrary to the expected behaviour. Little investigation into the CR model has been published, thus, the influence of χ_Z and ξ_Z on the position of IBs was investigated by employing the CR model in Python. LPPs from Nd:YAG lasers were the focus of the investigation, so n_e was set to 10^{-21} cm^{-3}. The results of the investigation were recently published [3], and a brief summary of the work is presented here.

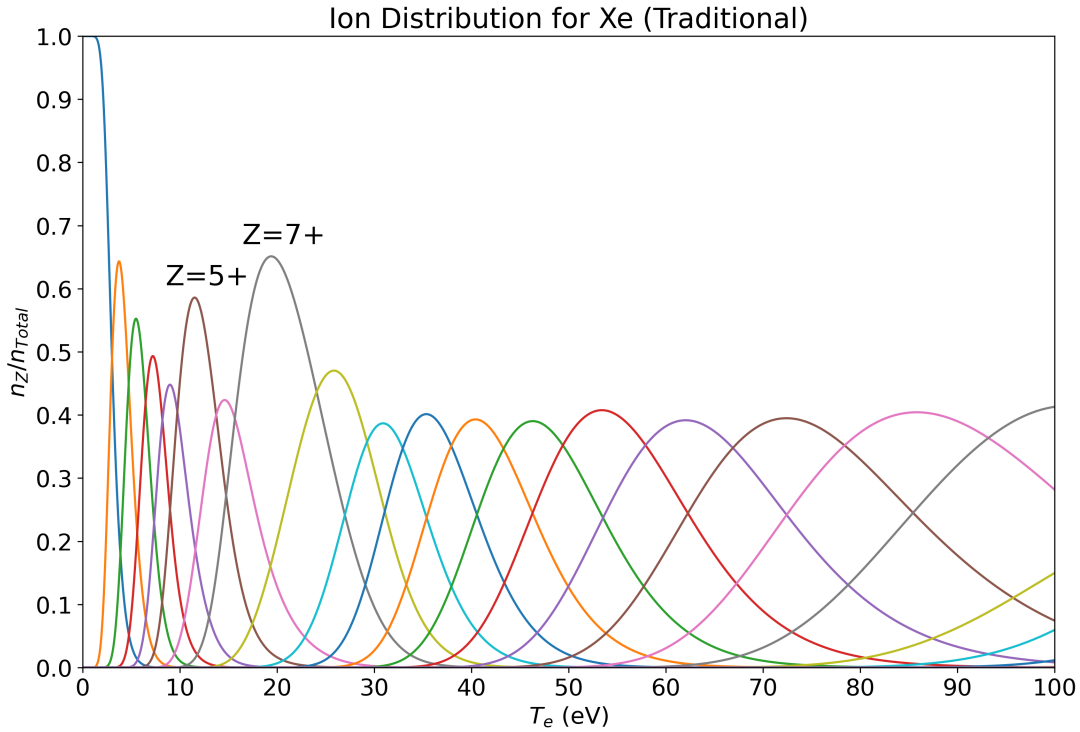

Figure 1: *Ion distribution for Xe. Each curve corresponds to a different ion stage, starting at* Xe^{0+} *on the left. The observed IBs* Xe^{5+} *and* Xe^{7+} *are labeled.*

First for the investigation, two different sets ofχ_Z values were employed either originating from the NIST database [4] or an approximate value from [1] and described as

$$\chi_Z \approx \frac{45Z^2}{Z_A^{2/3}} \quad [\text{eV}], \tag{5}$$

where χ_Z is the ionization energy in eV, Z is the charge, and Z_A is the atomic number of the element. Within the presented plots, the χ_Zs utilized in the calculation are denoted by NIST χ_Z when the database values are employed or CT χ_Z when Eq. (5) is employed. Second, either ξ_Z was included or not. ξ_Z was determined via the standard electron removal method, except in the lanthanides where $4f$ contraction was taken into account following the ion stage configurations presented in [5]. Finally, the peak fractional ion population as a function of the number of electrons and rate coefficients as a function of T_e were investigated along with the ion distributions for the determination of trends across the periodic table. Elements examined in the investigation ranged from C to U ($Z_A = 6$ to 82).

During the initial stages of the investigation a discrepancy was discovered in the radiative recombination rate coefficient, Eq. (3). A $1/2$ was originally a $1/3$ power in the source for Eq. (3) [6] and no reason for the change was discovered, and the corrected form of Eq. (3) is

$$\alpha_r(Z,T_e) = 5.2\times10^{-14}(\frac{T_e}{\chi_Z})^{1/2}Z[0.429+\frac{1}{2}\ln(\frac{\chi_Z}{T_e})+0.469(\frac{T_e}{\chi_Z})^{1/3}] \quad [\text{cm}^3\cdot\text{s}^{-1}], \tag{6}$$

where all of the variables are the same as before. When Eq. (6) replaced Eq. (3), the CR model produced ion distributions with curves shifted to slightly higher T_es, so the corrected radiative recombination rate coefficient was employed for the majority of calculations. For the plots, the notation of traditional or standard denotes the use of Eq. (3) or Eq. (6), respectively.

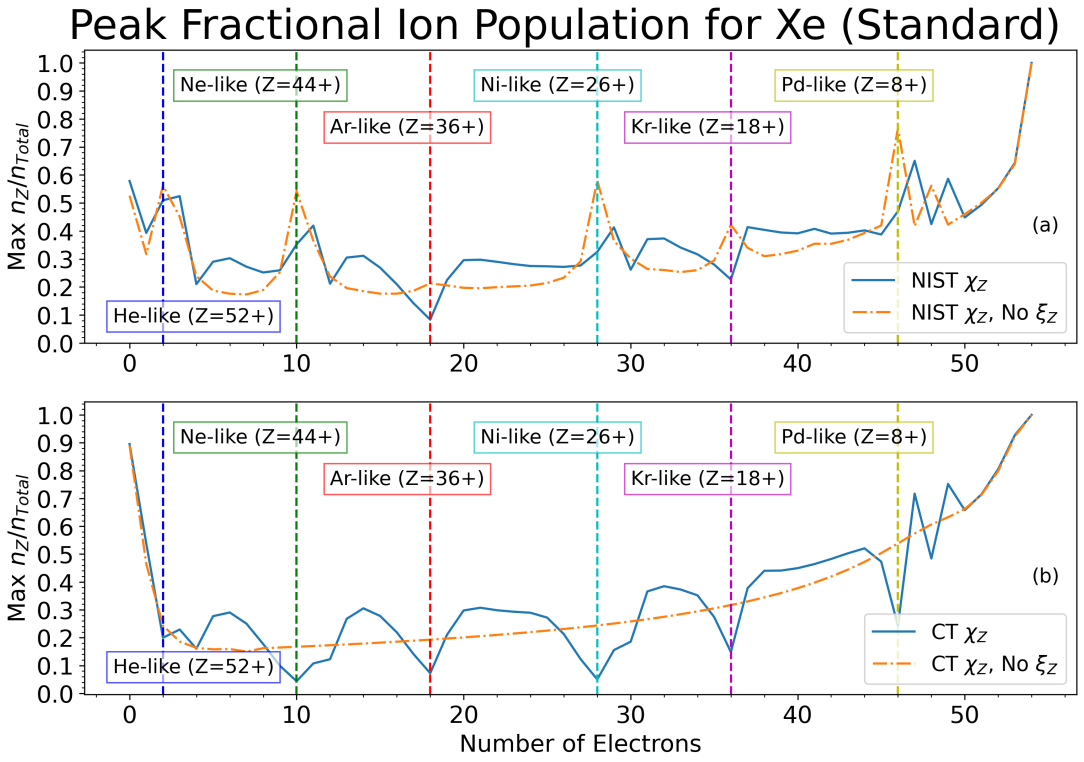

Figure 2: *Plots of the peak fractional ion population for Xe. The solid lines correspond to calculations including ξ_Z, while the dashed did not. Additionally, each ξ_Z case was employed with NIST χ_Zs (a) or CT χ_Zs (b). The vertical lines mark expected IBs corresponding to noble gas and filled nd^{10} outermost subshell configurations*

The elements exhibited common trends. Fig. (2) and Fig. (3) show the peak fractional ion population and collisional ionization rate coefficient plots for Xe, which are exemplary for many of the trends. For the peak fractional ion population plots, the sharp peaks indicated IBs, and across the elements examined, use of ξ_Z with either χ_Z resulted in expected IBs either being shifted to neighboring ion stages or being dips instead, as shown by the solid lines in Fig. (2). When ξ_Z was removed, the expected IBs were observed in calculations with the NIST χ_Zs, but all observed IB behaviour was smoothed in calculations with the CT χ_Zs, as shown by the dashed lines in Fig. (2). For the rate coefficients, the collisional ionization and three-body recombination curves displayed unexpected ion stage behavior, namely curves crossing and curves being out of order. Removal of the ξ_Z term removed the unexpected behavior as shown in Fig. (3). The radiative recombination plots did not contain the unexpected behavior, because the rate co-

effient, Eq. (6) does not contain ξ_Z. Deviations from these trends occurred in the lanthanides, however $4f$ contraction is thought to be the main cause of the differences. The phenomenon causes the value of ξ_Z to be ambiguous as the outermost electron subshell is no longer easily determinable [5]. Thus, ions with the same number of electrons as full orbital configurations (e.g. Xe-like) no longer exhibit closed shell behaviour. Examining the trends across the periodic table, the results as detailed in [3] are that the NIST χ_Zs without ξ_Z produce plots with the most expected behavior and proper care should be taken when choosing appropriate χ_Z and ξ_Z values to use with the CR model. While future plans in [3] included experimental comparisons and the inclusion of additional processes like photoionization, only the high temperature limit of the CR model has been under current investigation to better understand the applicability of the CR model for plasmas containing nearly bare ions.

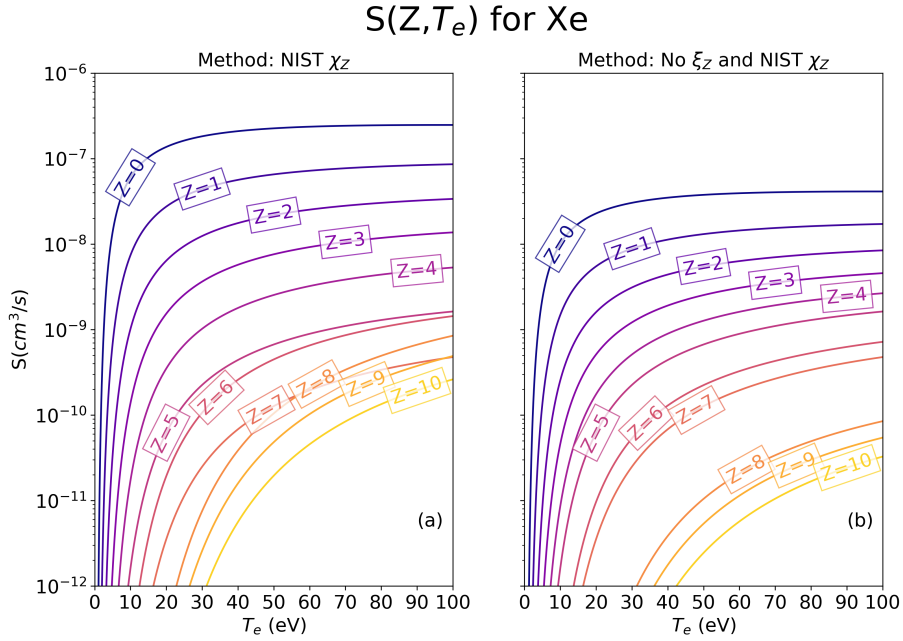

Figure 3: *Plots of the collisional ionization rate coefficient, Eq. (2), for Xe^{0+} to Xe^{10+} with the NIST χ_Zs. The left panel included ξ_Z (a), while the right panel did not (b).*

References

[1] D. Colombant and G.F. Tonon, J. Appl. Phys. **44**, 3524-3537 (1973)

[2] D.T. Attwood, A. Sakdinawat and L. Geniesse, X-rays and extreme ultraviolet radiation: principles and applications. 2nd ed. Cambridge University Press (2016)

[3] N.L. Wong, F. O'Reilly, and E. Sokell, Atoms. **8**, 52 (2020)

[4] A. Kramida, Y. Ralchenko, J. Reader, and NIST ASD Team, NIST Atomic Spectra Database (ver. 5.7.1.). National Institute of Standards and Technology

[5] D. Kilbane and G. O'Sullivan, Phys. Rev. A At. Mol. Opt. Phys. **82** 6 (2010)

[6] M.J. Seaton, Mon. Not. R. Astron. Soc. **119** 81-89 (1959)